

Reaction Mechanisms of Metal–Metal Bonded Carbonyls. X.¹ Thermal Decomposition of Decacarbonyldimanganese and Decacarbonylmanganeserhenium in Decalin²

J. Paul Fawcett, Anthony Poë,* and Kumud R. Sharma

Contribution from Erindale College and the Department of Chemistry, University of Toronto, Toronto, Canada. Received July 18, 1974

Abstract. The thermal decomposition of decacarbonyldimanganese in decalin, in the absence of oxygen and over a range of oxygen concentrations, has been studied in some detail. In the absence of oxygen the reaction is half-order in $[\text{Mn}_2(\text{CO})_{10}]$ over the range $(2\text{--}350) \times 10^{-5} M$ but decomposition under $\text{O}_2\text{--N}_2$ mixtures shows a transition from first- to half-order as $[\text{Mn}_2(\text{CO})_{10}]$ is increased from 1 to $500 \times 10^{-5} M$. The results are fully consistent with initial slow homolytic fission to form $\text{Mn}(\text{CO})_5$ radicals that can rapidly either recombine or react further to form decomposition products. Similar behavior is found with decacarbonylmanganeserhenium, and the activation parameters for the rate-limiting steps therefore provide a kinetic measure of the strength of the metal–metal bonds.

The mechanisms of reactions of dimanganese decacarbonyl have been a matter of some uncertainty. Wawersik and Basolo studied several substitution reactions in xylene of the decacarbonyl and some of its simple derivatives and concluded that their results were fully consistent with a simple dissociative mechanism.³ Poë et al. studied substitution reactions of the decacarbonyl in decalin, and also the thermal decomposition under atmospheres of nitrogen, air, and pure oxygen.⁴ Limiting rate constants for substitution by triphenylphosphine were appreciably higher than those obtained under oxygen unless the substitutions were performed under an atmosphere of carbon monoxide when the limiting rate constants for the two reactions appeared to be identical at all temperatures. It was concluded that the substitutions do proceed in part by a CO-dissociative path (completely inhibited by 1 atm of carbon monoxide) but that an additional path is available for substitution and for thermal decomposition in the presence or absence of oxygen. It was proposed that this path involves significant Mn–Mn bond breaking in the transition state. Similar results were also obtained for reactions of dirhenium decacarbonyl but the importance of the CO-inhibited path for substitution was much less in that case.⁵

Since the thermal decomposition reactions appeared to provide evidence of a rather different kind from the substitutions, we have extended their study considerably, and have shown that a simple CO-dissociative mechanism cannot possibly explain the results. The data are, however, in excellent agreement with a mechanism involving initial, slow homolytic fission of the Mn–Mn bond to form $\text{Mn}(\text{CO})_5$ radicals, which can then either recombine or react further in some way. Similar results are also reported for reactions of decacarbonylmanganeserhenium.

Experimental and Results

Baker Analyzed decalin was dried over molecular sieves and used without further treatment. Decacarbonyldimanganese (Strem Chemicals, Inc.) was recrystallized from hexane. Decacarbonylmanganeserhenium was prepared by the reaction⁶ of $\text{Re}(\text{CO})_5\text{Cl}$ with $\text{NaMn}(\text{CO})_5$ in freshly distilled anhydrous tetrahydrofuran. Kinetic runs were performed by standard techniques,⁷ degassing by repeated freeze–pump–thaw cycles, and the use of high purity gases (Argon, 99.998%, from Union Carbide of Canada, Ltd., and carbon monoxide, <20 ppm oxygen, from Matheson of Canada, Ltd.), ensuring the complete absence of oxygen when necessary. CO--N_2 and $\text{O}_2\text{--N}_2$ mixtures of composition known to $\pm 2\%$ were also obtained from Matheson of Canada, Ltd. When reactions were carried out under individually prepared mixed atmospheres of

oxygen and nitrogen or carbon monoxide the gas mixtures were contained in 20-cm³ individually ground syringes, the needles of which were inserted into the reaction vessel through the rubber septum cap; the samples were ejected as required by depressing the plunger. Reactions under air, 5%, and 100% oxygen were carried out under a slow continuous stream of gas. Otherwise reactions were carried out under atmospheres of gases from cylinders, samples being expressed at suitable times by applying a pressure of the gas. Spectra of the solutions were measured either in the C–O stretching region of the ir with a Perkin-Elmer 257 spectrophotometer or in the uv–visible region with a Cary 16 recording spectrophotometer. Matched pairs of ir cells were used, the path-lengths being measured either by the interference method or by use of the spectrum of benzene.

Thermal Decomposition of Decacarbonyldimanganese under an Inert Atmosphere. This reaction proceeds at conveniently detectable rates above ca. 80°C with complete loss of all absorption in the C–O stretching and uv–visible regions, the only product being a finely divided black precipitate presumably of manganese metal. Plots of $\log A$ vs. time (A = absorbance in ir or uv–visible) showed pronounced curvature, the gradient increasing with time, but plots of $A^{1/2}$ vs. time were linear for up to ca. 60% reaction before the gradient increased. The order of reaction with respect to [complex] was determined at 155°C under argon, and at 170°C under carbon monoxide, by measuring the initial rates R_0 as a function of initial concentration C_0 . Reactions were all followed over the first 10% reaction and initial rates obtained by multiplying $C_0^{1/2}$ by the half-order rate constants obtained from $A^{1/2}$ vs. time plots, this being a more precise way of obtaining values of R_0 than measurements of initial gradients of A vs. time plots even if the reaction had not turned out to be half-order in [complex]. Plots of $\log R_0$ vs. $\log C_0$ give good straight lines of gradient 0.5 as shown in Figure 1.

Data for the temperature dependence of $k_{1/2}(\text{obsd})$, either under argon or under oxygen-free carbon monoxide, are shown in Table I. Figure 2 shows that the Eyring plot is linear only up to ca. 140°C unless the reactions above 140°C are carried out under an atmosphere of carbon monoxide. In the absence of carbon monoxide the values of $\log(k_{1/2}/T)$ lie above the Eyring plot but the data at 170°C show that only quite small amounts of carbon monoxide are necessary to reduce the rates to those that fall on the linear plot. The standard deviation of $\pm 20\%$ derived for an individual measurement of $k_{1/2}$ is consistent with the scatter of the data in Figure 1.

Decomposition of $\text{Mn}_2(\text{CO})_{10}$ in the Presence of Oxygen. Reaction with oxygen in decalin leads to complete loss of absorption due to the terminal C–O stretching bands of $\text{Mn}_2(\text{CO})_{10}$ and to the formation of a flocculent black precipitate of manganese oxide.⁴ Ir bands at 1742 vs and 1704 cm^{-1} are also seen to grow, together with a broad weak band at 1600 cm^{-1} . Absorption also grows in the near-uv and this, combined with the formation of a relatively bulky precipitate, made observation of the reaction by uv–vis spec-

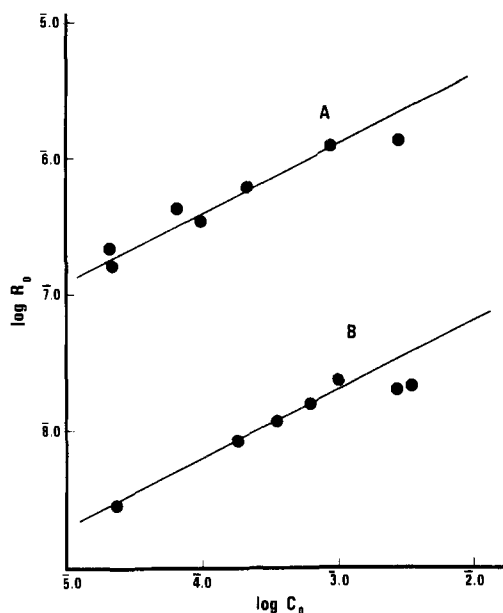


Figure 1. Dependence of initial rates of decomposition of $\text{Mn}_2(\text{CO})_{10}$ in decalin (A) under carbon monoxide at 170°C (abscissa is $(\log R_0 - 2)$) and (B) under argon at 155°C .

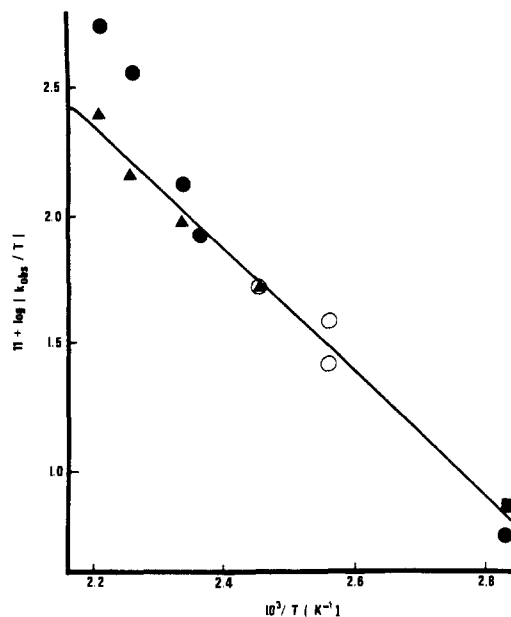


Figure 2. Temperature dependence of the half-order rate constant for decomposition of $\text{Mn}_2(\text{CO})_{10}$ in decalin: ●, under nitrogen or argon; ▲, under 1 atm of carbon monoxide; ○, from ref 8; ■, calculated from data in ref 9.

trospecty over the whole of its course very difficult. However, the first 10% reaction was easy to follow so that measurement of R_0 as a function of C_0 at 120°C was quite straightforward. The reaction could be followed over a longer time by observing the decrease in absorption due to the C-O stretching bands of the complex.

Dependence of the rates at 125°C on the pressure of oxygen above the reacting solutions was also studied and the observed pseudo-first-order rate constants were found to rise towards a limiting value. Excellent first-order plots, linear for over three half-lives, were found near the limiting rates but the plots became increasingly curved as the rates fell more below the limiting values. Even half-order plots under these conditions showed increasing rates towards the end of the reaction. One run at less than the limiting rate was allowed to undergo ca. 50% reaction (under conditions such that the rate was substantially less than the limiting rate) before being diluted with fresh reactant solution. The subsequent rate was found to be the same as that found for solutions of

Table I. Temperature Dependence of $k_{1/2}(\text{obsd})$ for Thermal Decomposition of $\text{Mn}_2(\text{CO})_{10}$ in the Absence of Oxygen. $[\text{Mn}_2(\text{CO})_{10}]_0 = 4 \times 10^{-4} M$

Temp, $^\circ\text{C}$	$p(\text{CO})^a$	$10^7 k_{1/2}(\text{obsd}), \text{L}^{1/2} \text{mol}^{-1/2} \text{sec}^{-1}$
180	0	25.0
180	1.0	11.3
170	0	15.8
170	0.051	7.4
170	0.27	6.2
170	1.0	6.4
155	0	5.6
155	1.0	4.0
150	0	3.6
135	0	2.1 ^b
135	1.0	2.1
115	0	1.00 ^b
115	0	1.47 ^b
80	0	0.175 ^{c,d}
80	0	0.133 ^d

$\Delta H_{1/2}^\ddagger = 11.1 \pm 0.5^e \text{ kcal mol}^{-1} (46.4 \pm 2.1 \text{ kJ mol}^{-1})$
 $\Delta S_{1/2}^\ddagger = -62.4 \pm 1.2 \text{ cal K}^{-1} \text{ mol}^{-1} (-261 \pm 5 \text{ J K}^{-1} \text{ mol}^{-1})$
 $\sigma(k_{1/2}) = \pm 20\%$

^a Mole fraction of carbon monoxide in CO-N₂ mixtures. ^b Calculated by converting the apparent first-order rate constants⁸ into initial rates, and thence into half-order rate constants, using the known values of $[\text{Mn}_2(\text{CO})_{10}]_0$. ^c Calculated from data⁹ where $[\text{Mn}_2(\text{CO})_{10}]_0 = 1.5 \times 10^{-3} M$ and $R_0 = 6.78 \times 10^{-10} \text{ mol L}^{-1} \text{ sec}^{-1}$. Rates were the same in benzene, ethyl acetate, and methyl methacrylate. ^d These values were corrected as described in the discussion before being used for calculation of the activation parameters. ^e Activation parameters are from rates under ≥ 0.27 atm of carbon monoxide or from those not affected by its presence. All uncertainties are standard deviations estimated by assuming all values of $k_{1/2}$ have the same percentage uncertainty.

the same complex concentration but without the presence of decomposition product. Another run was performed at a value of $p(\text{O}_2)$ such that the rate was expected to be substantially lower than the limiting rate but with carbon monoxide instead of nitrogen as the other gas in the mixture. The rate observed was not significantly lower than that expected for a corresponding oxygen-nitrogen mixture.

Because of the possible decrease in order of reaction with respect to [complex] as $p(\text{O}_2)$ is decreased, the data are all expressed in Table II in terms of initial rates obtained by multiplying the apparent first-order rate constants (from initial gradients of the log A vs. time plots) by C_0 rather than by measuring the initial gradients of the A vs. time plots.

Decomposition of $\text{MnRe}(\text{CO})_{10}$ in the Presence of Oxygen. This reaction went to completion under all conditions used, and no ir bands due to a product were seen to grow apart from a broad band at 1720 cm^{-1} . The formation of this product appears to be more pronounced than that occurring during the reaction of $\text{Mn}_2(\text{CO})_{10}$ and was associated with increased absorption in the uv which made following the reaction by uv-vis spectroscopy more difficult. Most of the reactions were followed by monitoring the decreasing absorbance of the ir band of the decacarbonyl at 2054 cm^{-1} .

At 110°C , decomposition reactions under both air and pure oxygen gave first-order plots that were linear for about 80% reaction, the rate constants being the same, and equal to those for the substitution reactions¹⁰ with triphenylphosphine. At 125°C , the reaction under air is slower than that under pure oxygen but the latter still has the same rate as the substitution reaction. Above 125°C the reactions under air and pure oxygen become increasingly slow compared with the limiting rate shown by the substitution reactions so that only the latter follow good Arrhenius behavior.¹⁰ It appears, therefore, that the reaction with oxygen approaches a limiting rate at high values of $p(\text{O}_2)$ that is equal to the rate of substitution, but that this limiting rate is not reached under 1 atm of oxygen at the higher temperatures.

The first-order rate plots show increasing curvature as the rates become progressively slower compared with the limiting rates. This suggests that the order of the reaction with respect to $[\text{MnRe}(\text{CO})_{10}]$ decreases as the rate decreases so all the data in Table III are given in terms of initial rates.

Table II. Initial Rates of Reaction of $\text{Mn}_2(\text{CO})_{10}$ with Oxygen in Decalin at 125°C

$10^5 C_0, M$	$p(\text{O}_2)^a$	$10^8 R_0, \text{mol l}^{-1} \text{sec}^{-1}$	$10^8 R_0$ (calcd), ^b $\text{mol l}^{-1} \text{sec}^{-1}$	$100[R_0 - R_0]/R_0$ (calcd) – (calcd)
1.51	0.053	0.32 ^c	0.44	27.2
3.22	0.053	0.74 ^c	0.78	5.1
3.66	0.053	0.99 ^c	0.86	-15.1
5.94	0.053	0.89 ^d	1.21	26.4
7.90	0.053	1.39 ^d	1.46	4.8
14.6	0.053	2.66 ^d	2.16	-23.1
28.8	0.053	3.22 ^d	3.24	0.6
50.0	0.053	4.85 ^e	4.46	-8.7
50.0	0.053	5.11 ^e	4.46	-14.6
56.8	0.053	4.72 ^e	4.79	1.5
58.2	0.053	5.27 ^d	4.86	-8.4
102	0.053	6.20 ^{e,f}	6.62	6.3
117	0.053	6.74 ^d	7.13	5.5
240	0.053	8.59 ^f	10.5	18.2
340	0.053	10.2 ^e	12.6	19.0
473	0.053	9.84 ^e	14.9	33.9
530	0.053	9.06 ^e	15.9	43.0
580	0.053	11.7 ^e	16.6	29.5
602	0.053	19.3 ^e	17.0	-13.5
1.03	0.21	0.31 ^c	0.40	24.4
1.05	0.21	0.25 ^c	0.40	37.5
1.40	0.21	0.32 ^c	0.52	38.5
3.35	0.21	1.52 ^c	1.20	-26.7
3.75	0.21	1.10 ^c	1.30	15.4
4.68	0.21	2.0 ^c	1.60	-25.0
9.0	0.21	2.54 ^c	2.80	9.3
18.4	0.21	5.24 ^c	4.94	-6.1
27.8	0.21	6.14 ^c	6.70	8.4
32.0	0.21	7.06 ^f	7.46	5.4
32.0	0.21	6.91 ^f	7.46	7.4
38.6	0.21	8.54 ^f	8.80	3.0
56.3	0.21	7.42 ^c	11.0	32.5
70.7	0.21	12.4 ^c	12.8	3.1
106	0.21	17.5 ^c	16.6	-5.4
167	0.21	17.5 ^g	21.8	19.7
169	0.21	17.5 ^g	21.9	20.1
202	0.21	20.7 ^h	24.4	15.2
280	0.21	27.9 ⁱ	29.6	5.7
368	0.21	29.2 ^j	33.0	11.5
513	0.21	39.0 ^f	41.8	6.7
1.51	1.0	0.48 ^c	0.59	18.4
5.42	1.0	2.10 ^c	2.11	0.47
10.2	1.0	4.0 ^c	3.91	-2.3
23.8	1.0	7.7 ^c	9.2	16.4
32.0	1.0	12.5 ^f	11.9	-5.0
32.0	1.0	12.2 ^f	11.9	-2.5
32.0	1.0	11.0 ^f	11.9	7.5
34.3	1.0	13.2 ^f	12.5	-5.6
34.9	1.0	12.9 ^c	12.9	0
105	1.0	25.0 ^f	35.4	29.4
167	1.0	49.0 ^g	52.7	7.0
167	0.78	50.0 ^g	51.9	3.7
32.0	0.60	11.0 ^f	11.0	0
167	0.51	28.0 ^g	39.3	28.7
32.0	0.40	9.69 ^f	9.9	2.1
167	0.18	19.0 ^g	19.4	2.1
32.0	0.15	5.36 ^f	6.14	12.7
32.0	0.11	5.62 ^f	5.03	-11.7
32.0	0.068	3.48 ^f	3.62	3.9

^a $p(\text{O}_2)$ = mole fraction of oxygen in O_2 - N_2 mixtures, ^bCalculated as described in Discussion, ^cFollowed at 343 nm (ϵ 21500 l. mol⁻¹ cm⁻¹), ^dFollowed at 2012 cm⁻¹ (ϵ 48300 l. mol⁻¹ cm⁻¹), ^eFollowed at 1980 cm⁻¹ (ϵ 7250 l. mol⁻¹ cm⁻¹), ^fFollowed at 2047 cm⁻¹ (ϵ 13200 l. mol⁻¹ cm⁻¹), ^gFollowed at 353 nm (ϵ 16800 l. mol⁻¹ cm⁻¹), ^hFollowed at 359 nm (ϵ 12200 l. mol⁻¹ cm⁻¹), ⁱFollowed at 363 nm (ϵ 10000 l. mol⁻¹ cm⁻¹), ^jFollowed at 369 nm (ϵ 8000 l. mol⁻¹ cm⁻¹).

Discussion

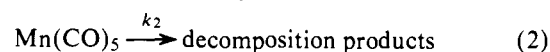
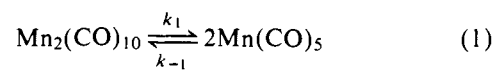
Thermal Decomposition of $\text{Mn}_2(\text{CO})_{10}$ under Argon. The half-order dependence on $[\text{Mn}_2(\text{CO})_{10}]$, the absence of in-

Table III. Initial Rates of Reaction of $\text{MnRe}(\text{CO})_{10}$ with Oxygen in Decalin

Temp, °C	$10^5 C_0, M$	$p(\text{O}_2)^a$	$10^8 R_0, \text{mol l}^{-1} \text{sec}^{-1}$	$10^8 R_0$ (calcd), ^b $\text{mol l}^{-1} \text{sec}^{-1}$	$100[R_0 - R_0]/R_0$ (calcd) – (calcd)
155	1.80	0.21	2.11 ^c	2.14	1.4
155	2.22	0.21	2.33 ^d	2.56	8.9
155	4.07	0.21	3.91 ^d	4.22	7.3
155	9.65	0.21	6.47 ^c	8.07	19.8
155	16.6	0.21	13.7 ^c	11.7	-17.1
155	89.7	0.21	33.3 ^c	33.3	0
155	238	0.21	61.0 ^e	57.4	-6.3
155	342	0.21	74.5 ^f	70.0	-6.4
155	39.0	0.115	13.6 ^d	12.3	-10.6
155	39.0	0.21	21.8 ^d	20.3	-7.4
155	39.0	0.21	23.0 ^d	20.3	-13.3
155	39.0	0.30	29.2 ^{d,g}	26.2	-11.5
155	39.0	0.59	38.8 ^d	38.7	-0.3
155	39.0	1.0	40.0 ^d	46.6	14.2
155	39.0	1.0	41.0 ^d	46.6	12.0
155	39.0	1.0	42.8 ^d	46.6	8.1
155	141	1.0	127 ^c	132	3.8
140	40	1.0	227 ^d		
140	40	1.0	230 ^d		
140	40	0.21	170 ^d		
125	40	1.0	40.4 ^d		
125	40	1.0	37.1 ^d		
110	40	1.0	5.40 ^d		
110	40	1.0	5.37 ^d		
110	40	0.21	5.30 ^d		

^aMole fraction of oxygen in O_2 - N_2 mixtures, ^bCalculated as described in Discussion, ^cFollowed at 324 nm (ϵ 14500 l. mol⁻¹ cm⁻¹), ^dFollowed at 2054 cm⁻¹ (ϵ 6700 l. mol⁻¹ cm⁻¹), ^eFollowed at 335 nm (ϵ 12800 l. mol⁻¹ cm⁻¹), ^fFollowed at 350 nm (ϵ 8300 l. mol⁻¹ cm⁻¹), ^gReaction under 30:70 O_2 -CO mixture.

hibition by carbon monoxide at lower temperatures, and the linearity of the Eyring plot when the reactions at higher temperatures proceed under carbon monoxide all show that the major reaction path cannot involve initial slow CO dissociation. An attractive, simple alternative is shown in eq 1 and 2



for which a steady-state treatment leads to the rate law in eq 3

$$-dC/dt = R = 2k_1 C / \{1 + (1 + aC)^{1/2}\} \quad (3)$$

where $C = [\text{Mn}_2(\text{CO})_{10}]$ and $a = 16k_1 k_{-1} / k_2^2$. The data are in good agreement with this equation. Thus, when $aC \approx 10^2$, eq 3 simplifies to eq 4

$$R = (2k_1 / a^{1/2}) C^{1/2} = 0.5(k_1 / k_{-1})^{1/2} k_2 C^{1/2} \quad (4)$$

in accordance with the half-order behavior shown by the initial rate studies of the decomposition at 155°C under argon and 170°C under carbon monoxide. Although half-order rate plots were appreciably more linear than first-order ones they still showed an acceleration over the last 40% of the reaction. It is presumed that autocatalysis by very finely divided metallic decomposition products is probably causing this acceleration.

Although half-order behavior was observed at 155 and 170°C, it is necessary to check that it is followed at all other temperatures at which the reaction was studied before the temperature dependence of the values of $k_{1/2}(\text{obsd})$ in Table I can be analyzed. This check can be made quite simply by rearranging eq 3 to give eq 5

$$a = (4k_1/R_0^2)(R_1 - R_0) \quad (5)$$

where R_0 is the observed initial rate and $R_1 = k_1C_0$ is assumed to be given by the limiting rate under pure oxygen. At 80°C, $k_1 = 8.9 \times 10^{-7} \text{ sec}^{-1}$ and R_0 for $C_0 = 1.5 \times 10^{-3} M^9$ can be calculated to be $6.78 \times 10^{-10} \text{ mol l}^{-1} \text{ sec}^{-1}$ in benzene,¹¹ from which we obtain $a = 5.1 \times 10^3 \text{ l. mol}^{-1}$. The half-order rate constant (corresponding to the limiting conditions) is calculated from eq 4 to be $2.5 \times 10^{-8} \text{ mol}^{1/2} \text{ l.}^{-1/2} \text{ sec}^{-1}$ as compared to the value of $k_{1/2}(\text{obsd})$ in Table I of $1.8 \times 10^{-8} \text{ mol}^{1/2} \text{ l.}^{-1/2} \text{ sec}^{-1}$. Similarly our own data for reaction in decalin at 80°C lead to $a = 8.5 \times 10^3 \text{ l. mol}^{-1}$ and $k_{1/2} = 1.9 \times 10^{-8} \text{ mol}^{1/2} \text{ l.}^{-1/2} \text{ sec}^{-1}$ as compared to $k_{1/2}(\text{obsd}) = 1.13 \times 10^{-8} \text{ mol}^{1/2} \text{ l.}^{-1/2} \text{ sec}^{-1}$. Evidently the limiting condition for true half-order behavior, $aC_0 \geq 10^2$, does not apply at 80°C, and we have used corrected values of $k_{1/2}(\text{obsd})$ in Figure 2 and in calculating the activation parameters in Table I. The difference between $k_{1/2}$ and $k_{1/2}(\text{obsd})$ is greater for the more dilute solution of complex where half-order behavior is expected to be less closely approached. This type of calculation was repeated with data at all the other temperatures used and limiting half-order conditions were found to apply.

According to eq 4 and Table I, $\Delta H_{1/2}^\ddagger = \Delta H_2^\ddagger + 0.5(\Delta H_1^\ddagger - \Delta H_{-1}^\ddagger) = 11.1 \pm 0.5 \text{ kcal mol}^{-1}$, and $\Delta S_{1/2}^\ddagger = \Delta S_2^\ddagger + 0.5(\Delta S_1^\ddagger - \Delta S_{-1}^\ddagger) - R \ln 2$ so that $\Delta S_2^\ddagger + 0.5(\Delta S_1^\ddagger - \Delta S_{-1}^\ddagger) = -61.0 \pm 1.2 \text{ cal K}^{-1} \text{ mol}^{-1}$. Data of Segal et al.¹² led to a value of $E_a = 16 \pm 2 \text{ kcal mol}^{-1}$ for the gas-phase decomposition of $\text{Mn}_2(\text{CO})_{10}$ observed manometrically from 240 to 310°C. Although they claimed to observe first-order kinetics this value is much closer to our value of $\Delta H_{1/2}^\ddagger$ than to the $36.8 \pm 0.4 \text{ kcal mol}^{-1}$ value of ΔH_1^\ddagger obtained from Haines' data.⁸ Unfortunately, no values are given for the "concentration" of $\text{Mn}_2(\text{CO})_{10}$ in Segal's experiments although first-order plots of his data show the curvature expected if the reactions were in fact half-order in $[\text{Mn}_2(\text{CO})_{10}]$.

Bidinosti and McIntyre¹³ obtained a value of $\Delta H_1^\circ = \Delta H_1^\ddagger - \Delta H_{-1}^\ddagger = 25 \pm 2 \text{ kcal mol}^{-1}$ by mass spectrometric studies of the presumed equilibrium $\text{Mn}_2(\text{CO})_{10} \rightleftharpoons 2\text{Mn}(\text{CO})_5$ from 210 to 310°C. If this gas-phase value is accepted as an approximate measure of the value in the inert solvent decalin we obtain $\Delta H_{-1}^\ddagger = \text{ca. } 12 \text{ kcal mol}^{-1}$ and $\Delta H_2^\ddagger = \text{ca. } -1 \text{ kcal mol}^{-1}$. No value of ΔS_1° is known so we cannot estimate either ΔS_{-1}^\ddagger or ΔS_2^\ddagger . The value of ΔH_{-1}^\ddagger implies that each $\text{Mn}(\text{CO})_5$ radical requires an average enthalpy of 6 kcal mol⁻¹ to attain the transition state for dimerization. This implies that the radicals are not simply in a C_{4v} configuration with the unpaired electron in an orbital along the C_{4v} axis, and a trigonal bipyramidal configuration seems more likely. The slightly negative value of ΔH_2^\ddagger would imply that reaction 2 is not a simple one-step reaction. Reaction with trace impurities in the solvent is possible and could account for the relatively modest precision of the data. Reaction with the solvent might also occur at some stage¹⁴ although if $\text{HMn}(\text{CO})_5$ were formed one might expect some evidence for hydrogen evolution through the reaction $2\text{HMn}(\text{CO})_5 \rightarrow \text{H}_2 + \text{Mn}_2(\text{CO})_{10}$. This was tested for¹⁵ by measuring both the Raman spectrum and the volume of the gas evolved when the reaction was allowed to proceed to 30-50% completion in the absence of inert gases above the solution. Only very slight traces of hydrogen (at most 5% of the evolved gas) were detected spectroscopically. The volume of the gas evolved was about 30% less than that expected if all the reacted decacarbonyl had decomposed completely. The concentration of complex used in these experiments was about ten times that used in the kinetic studies and it seems possible that formation of insoluble, perhaps hydridic, higher clusters occurred. These

must be unstable to air, since no C-O stretching bands were seen on measuring the ir of the insoluble product, but they could be involved as intermediates in the decomposition of the $\text{Mn}(\text{CO})_5$ radicals. However, the nature of the decomposition path or paths is certainly far from clear.

The high-temperature decomposition path that is readily inhibited by carbon monoxide probably does not involve simple CO dissociation from $\text{Mn}_2(\text{CO})_{10}$ since the initial rates are very much slower than the part of the substitution reaction that has been ascribed⁴ to this mechanism, and the amount of carbon monoxide liberated into the solution during the first 10% reaction would not be sufficient to bring this about. It seems more likely that the decomposition involves CO dissociation from $\text{Mn}(\text{CO})_5$ radicals as an additional path at high temperatures. This CO dissociation should have a significant value of ΔH^\ddagger so that it would compete more successfully with the other modes of decomposition of $\text{Mn}(\text{CO})_5$ at higher temperatures as is observed.

Thermal Decomposition of $\text{Mn}_2(\text{CO})_{10}$ under Oxygen.

This reaction leads to the formation of manganese oxide and appears to be accompanied, especially towards the end of the reaction, by oxidation of the solvent to form ketonic products. Although product solutions containing a suspension of oxide do not appear to catalyze the reaction of fresh solutions, the increase in rate towards the end of the reactions could well be caused by a more reactive form of the oxide produced before final coagulation.

The dependence of the initial rates on C_0 (Figure 3) shows that the reaction under air changes from being close to first order in $[\text{Mn}_2(\text{CO})_{10}]$ towards being half-order as $[\text{Mn}_2(\text{CO})_{10}]$ increases. Under an atmosphere of pure oxygen the first-order behavior is maintained until higher concentrations of complex, whereas under 5% oxygen the half-order behavior is maintained down to lower concentrations. The form of these results is exactly what would be expected for a mechanism shown by eq 1, 2, and 6



for which a steady-state treatment leads to the rate law shown in eq 7

$$R = (2k_1C)/\{1 + bC\}^{1/2} + 1\} \quad (7)$$

where $b = 16k_1k_{-1}/(k_2 + k_6[\text{O}_2])^2$. Reaction 6 must be fast enough for it to compete with the reverse of reaction 1 so that the order with respect to $[\text{Mn}_2(\text{CO})_{10}]$ can increase above 0.5, towards limiting first-order behavior, at low $[\text{Mn}_2(\text{CO})_{10}]$ and/or high $[\text{O}_2]$. Equation 7 can be rearranged to eq 8.

$$2R/(R_1 - R)^{1/2} = c = k_2/k_{-1}^{1/2} + k_6[\text{O}_2]/k_{-1}^{1/2} \quad (8)$$

To calculate R_1 , k_1 was taken to be $3.9 \times 10^{-4} \text{ sec}^{-1}$, a value obtained from the limiting rates of reaction under 1 atm of oxygen and at relatively low concentrations of complex. A plot of $2R_0/(R_1 - R_0)^{1/2}$ against $p(\text{O}_2)$ is shown in Figure 4, and is in excellent agreement with that expected from eq 8. The intercept, though possibly finite, is not precisely enough defined to compare with the value ca. $0.2 \times 10^{-4} \text{ mol}^{1/2} \text{ l.}^{-1/2} \text{ sec}^{-1/2}$ predicted by the data for the reaction in the absence of oxygen.

In order to express the data for varying concentrations of complex at constant $[\text{O}_2]$ eq 8 can conveniently be rearranged to eq 9

$$\log \{(k_1 - k_0)^{1/2}/k_0\} = 0.5 \log C_0 - \log c \quad (9)$$

where k_0 is the apparent pseudo-first-order rate constant obtained from the initial gradient of a plot of $\log(A - A_\infty)$ against time when the initial concentration of complex was

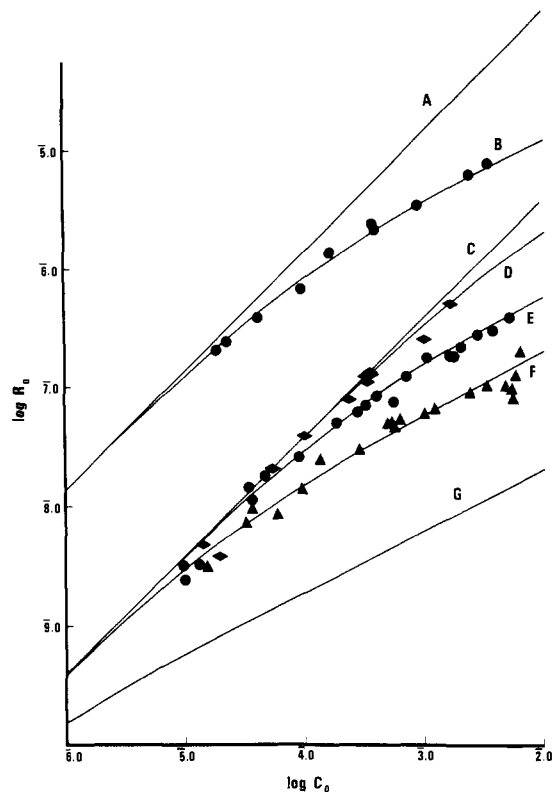


Figure 3. Dependence of initial rates of decomposition of $\text{Mn}_2(\text{CO})_{10}$ and $\text{MnRe}(\text{CO})_{10}$ in decalin under $\text{O}_2\text{-N}_2$ mixtures: A, $(\log R_1) - 1$ vs. $\log C_0$ for $\text{MnRe}(\text{CO})_{10}$ at 155°C ; B, $(\log R_0) - 1$ vs. $\log C_0$ for $\text{MnRe}(\text{CO})_{10}$ at 155°C and $p(\text{O}_2) = 0.21$; C, $\log R_1$ vs. $\log C_0$ for $\text{Mn}_2(\text{CO})_{10}$ at 125°C ; D, E, F, $\log R_0$ vs. $\log C_0$ at 125°C and $p(\text{O}_2) = 1.0, 0.21,$ and $0.053,$ respectively; G, calculated dependence of $\log R_0$ on $\log C_0$ under argon (i.e., $p(\text{O}_2) = 0$). All continuous lines are calculated using parameters as described in the text.

C_0 . Figure 5 shows the plots of $\log \{(k_1 - k_0)^{1/2}/k_0\}$ against $\log C_0$ for $p(\text{O}_2) = 0.053$ and 0.21 . Straight lines of gradient 0.5 pass very close to all but a few of the points. The plots lead to values of 2.0×10^{-4} and $6.2 \times 10^{-4} \text{ mol}^{1/2} \text{ l.}^{-1/2} \text{ sec}^{-1/2}$ for c when $p(\text{O}_2) = 0.053$ and 0.21 , respectively. The corresponding values of $[\text{O}_2]$ are 0.30 and 1.2 mM , respectively, based on measurements of 7.6 and 7.2 mM , respectively, at 30 and 70°C under 1 atm of oxygen and decalin vapor. These measurements^{10,16} were made by the method of Morrison and Billet¹⁷ and correction for the temperature difference was made by allowing only for the different vapor pressures of decalin;¹⁸ i.e., it was assumed that the heat of solution of oxygen in decalin is negligible. A negligible heat of solution of carbon monoxide in decalin has been found from 20 to 75°C .¹⁶ Since $k_2/k_{-1}^{1/2}$ is ca. $0.2 \times 10^{-4} \text{ mol}^{1/2} \text{ l.}^{-1/2} \text{ sec}^{-1/2}$ these two values of c lead to values of 0.59 and $0.50 \text{ l.}^{1/2} \text{ mol}^{-1/2} \text{ sec}^{-1/2}$, respectively, for $k_6/k_{-1}^{1/2}$, in good agreement with the value $0.52 \text{ l.}^{1/2} \text{ mol}^{-1/2} \text{ sec}^{-1/2}$ found from the gradient in Figure 4. The first two values have been used to calculate curves F and E, respectively, in Figure 3.

Taking the values $k_1 = 3.9 \times 10^{-4} \text{ sec}^{-1}$, $k_2/k_{-1}^{1/2} = 0.2 \times 10^{-4} \text{ mol}^{1/2} \text{ l.}^{-1/2} \text{ sec}^{-1/2}$, and values of $k_6/k_{-1}^{1/2}$ appropriate to the particular group of runs, values of R_0 were calculated from eq 7 for any value of C_0 and $p(\text{O}_2)$. These values are listed in Table II together with the corresponding values of $100[R_0(\text{calcd}) - R_0]/R_0(\text{calcd})$, the root mean square value of which is $\pm 17\%$. This is satisfactory precision in view of the 500-fold range of values of C_0 and the 20-fold range of $p(\text{O}_2)$.

The temperature dependence of the parameter k_{-1}/k_6^2 can be obtained by applying eq 8 to Haines' data⁸ for reac-

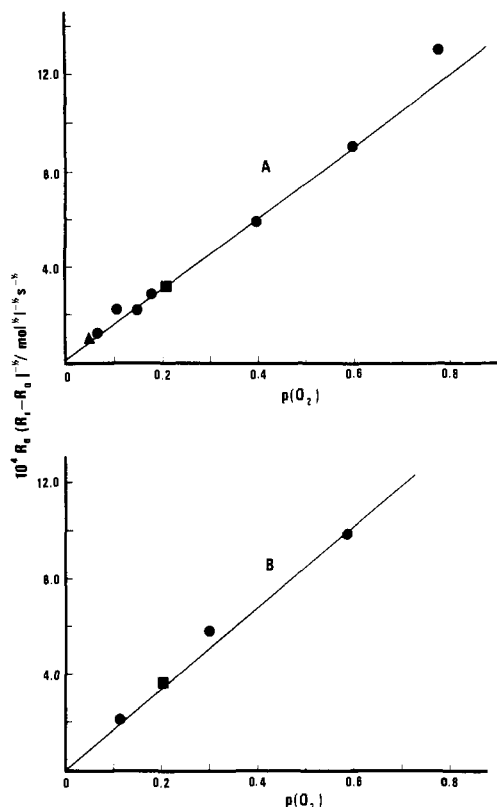
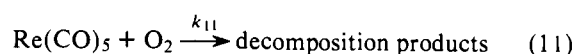
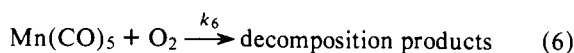
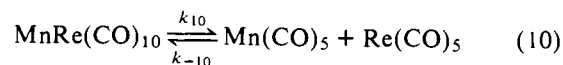


Figure 4. Dependence of initial rates on $p(\text{O}_2)$: A, $\text{Mn}_2(\text{CO})_{10}$ at 125°C ; ■, average of all data in Table II at $p(\text{O}_2) = 0.21$; ▲, average of all data in Table II at $p(\text{O}_2) = 0.053$; B, $\text{MnRe}(\text{CO})_{10}$ at 155°C ; ■, average of all data in Table III at $p(\text{O}_2) = 0.21$.

tion with oxygen and air. R_0 is obtained from $k_0[\text{Mn}_2(\text{CO})_{10}]$ where values of k_0 were obtained⁸ from initial slopes of first-order plots, and $k_2/k_{-1}^{1/2}$ was taken to be negligible. The data are shown in Table IV together with the activation parameters derived graphically. Using the value of ΔH_{-1}^\ddagger estimated earlier we obtain $\Delta H_6^\ddagger = \text{ca. } 8 \text{ kcal mol}^{-1}$. This value seems to be not unreasonable although no comparable data seem to be available. Again, since no value for ΔS_{-1}^\ddagger is known, we cannot estimate ΔS_6^\ddagger . The initial product of reaction 6 may be the adduct $\text{O}_2\text{Mn}(\text{CO})_5$ which has been identified¹⁹ by ESR measurements in the solid state at low temperatures, and which could be a catalyst for oxidation of the solvent.

Thermal Decomposition of $\text{MnRe}(\text{CO})_{10}$ under Oxygen.

The behavior of this reaction is identical with that of the dimanganese complex, a similar oxidation of the solvent and some form of autocatalysis appearing to occur. A plot of $\log R_0$ against $\log [\text{MnRe}(\text{CO})_{10}]_0$ is shown in Figure 3, and the dependence on $p(\text{O}_2)$ shows a rise towards a limiting rate, the rise being more rapid at lower temperatures. Even for a reaction going at about half the limiting rate a considerable pressure of carbon monoxide above the reacting solution has no further retarding effect. The observed behavior cannot, therefore, correspond to a CO-dissociative mechanism. It is consistent, however, with the mechanism shown in eq 10, 6, and 11.



The fact that no evidence is found for the formation of

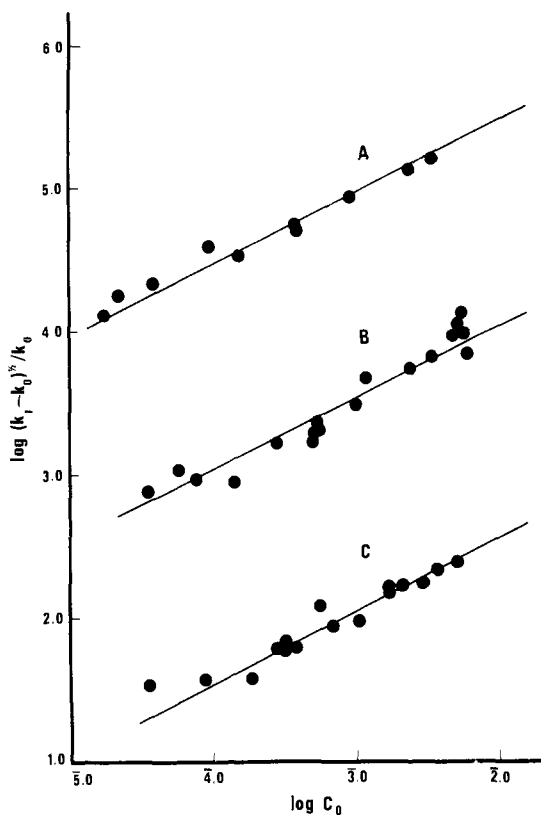


Figure 5. A, $3 + \log(k_1 - k_0)^{1/2}/k_0$ vs. $\log C_0$ for $\text{MnRe}(\text{CO})_{10}$ at 155°C and $p(\text{O}_2) = 0.21$; B, $1 + \log(k_1 - k_0)^{1/2}/k_0$ vs. $\log C_0$ for $\text{Mn}_2(\text{CO})_{10}$ at 125°C and $p(\text{O}_2) = 0.053$; C, $\log(k_1 - k_0)^{1/2}/k_0$ vs. $\log C_0$ for $\text{Mn}_2(\text{CO})_{10}$ at 125°C and $p(\text{O}_2) = 0.21$. All lines have gradient of 0.5.

$\text{Mn}_2(\text{CO})_{10}$ or $\text{Re}_2(\text{CO})_{10}$ during the reaction is surprising since $\text{Re}_2(\text{CO})_{10}$ is relatively stable towards reaction with oxygen under these conditions.⁵ This seems to imply that the reverse of reaction 10 must be more rapid than the reaction together of like radicals. Recent studies²⁰ have shown that $\text{Re}_2(\text{CO})_{10}$ and $\text{Mn}_2(\text{CO})_{10}$ are each formed in roughly 5% yield by the flash photolysis of $\text{ReMn}(\text{CO})_{10}$ in isooctane. This is believed to be due to photoinduced homolytic fission although it is not clear whether the remaining "unreacted" $\text{ReMn}(\text{CO})_{10}$ is genuinely unreacted or has been re-formed after homolytic fission. The latter is suggested by the very high yields of $\text{MnRe}(\text{CO})_{10}$ formed by photolysis of equimolar amounts of $\text{Mn}_2(\text{CO})_{10}$ and $\text{Re}_2(\text{CO})_{10}$. That the mixed complex might be thermodynamically favored over mixtures of the two unmixed complexes is also suggested by the greater than average strength of the Mn-Re bond (compared with the Mn-Mn and Re-Re bonds) as indicated by force constant,²¹ mass spectrometric,²² and kinetic data.^{10,23}

The rate law for the proposed mechanism is shown in eq 12

$$-dC/dt = R = 2k_{10}C/\{(1 + dC)^{1/2} + 1\} \quad (12)$$

where $C = [\text{MnRe}(\text{CO})_{10}]$ and $d = 4k_{10}k_{-10}/k_6k_{11}[\text{O}_2]^2$. The spontaneous decomposition of the $\text{Mn}(\text{CO})_5$ and $\text{Re}(\text{CO})_5$ radicals has been considered to contribute negligibly to the rate so that a plot of $\log(k_1 - k_0)^{1/2}/k_1$ against $\log C_0$, for reactions at $[\text{O}_2] = \text{constant}$, should be linear with a gradient of 0.5 and an intercept of $-\log(k_6k_{11}/k_{-10})^{1/2}[\text{O}_2]$. Such a plot for data at 155°C is shown in Figure 5 (k_1 taken as $1.4 \times 10^{-3} \text{ sec}^{-1}$),¹⁰ and leads to a value of $0.41 \text{ l.}^{1/2} \text{ mol}^{-1/2} \text{ sec}^{-1/2}$ for $(k_6k_{11}/k_{-10})^{1/2}$. A plot of $R_0/(R_1 - R_0)^{1/2}$ against $p(\text{O}_2)$, which should also

Table IV. Temperature Dependence of k_{-1}/k_6^2 for the $\text{Mn}_2(\text{CO})_{10}$ -Oxygen Reaction.^a $[\text{Mn}_2(\text{CO})_{10}] \approx 4 \times 10^{-4} M$

Temp, °C	$p(\text{O}_2)$	$10^3[\text{O}_2], M$	$10^5k_0, \text{sec}^{-1}$	$10^7R_1, \text{mol l.}^{-1} \text{sec}^{-1}$	$10^7R_0, \text{mol l.}^{-1} \text{sec}^{-1}$	$k_{-1}/k_6^2, \text{mol l.}^{-1} \text{sec}$
145	1.0		385 ^b	15.4		
145	0.21	1.0	79.8		3.2	3.1
135	1.0		122	4.9		
135	0.21	1.1	42.4		1.7	3.5
125	1.0			1.5		
125	0.21	1.2			0.67	4.0
115	1.0		12.0	0.48		
115	0.21	1.3	8.1		0.32	4.6

$\Delta H_{-1}^\ddagger - 2\Delta H_6^\ddagger = -3.5 \pm 1.0^c \text{ kcal mol}^{-1}$ ($-15 \pm 4 \text{ kJ mol}^{-1}$)
 $\Delta S_{-1}^\ddagger - 2\Delta S_6^\ddagger = 53 \pm 4^c \text{ cal K}^{-1} \text{ mol}^{-1}$ ($220 \pm 16 \text{ J K}^{-1} \text{ mol}^{-1}$)

^aData from ref 8. ^bExtrapolated from lower temperatures. ^cUncertainties are approximate estimates, made graphically, of the maximum error. The precision of k_{-1}/k_6^2 decreases with decreasing temperature.

be linear, is shown in Figure 4 and leads to a value of $0.43 \text{ l.}^{1/2} \text{ mol}^{-1/2} \text{ sec}^{-1/2}$ for $(k_6k_{11}/k_{-10})^{1/2}$. Values of the rates for all values of C_0 and $[\text{O}_2]$ can be calculated by using the above values of k_1 , and $(k_6k_{11}/k_{-10})^{1/2} = 0.42 \text{ l.}^{1/2} \text{ mol}^{-1/2} \text{ sec}^{-1/2}$. These rates are given in Table IV and lead to a root mean square deviation of the experimental from the calculated values of $\pm 10\%$. Curve B, Figure 3, was also calculated by using these parameters.

Values of R_{10} , and of R_0 under air, are also known at 140 and 125°C and values of k_6k_{11}/k_{-10} can be calculated to be 0.37 and 0.33 $\text{l. mol}^{-1} \text{ sec}^{-1}$, respectively. Values of $\Delta H_6^\ddagger + \Delta H_{11}^\ddagger - \Delta H_{-10}^\ddagger = 7 \text{ kcal mol}^{-1}$, and $\Delta S_6^\ddagger + \Delta S_{11}^\ddagger - \Delta S_{-10}^\ddagger = -47 \text{ cal K}^{-1} \text{ mol}^{-1}$ are obtained from an Eyring plot and are close to the corresponding values for the reaction of $\text{Mn}_2(\text{CO})_{10}$. Since $\Delta H_6^\ddagger = \text{ca. } 8 \text{ kcal mol}^{-1}$, $\Delta H_{-10}^\ddagger \approx \Delta H_{11}^\ddagger$.

Conclusions

Although the kinetic data could also be consistent with heterolytic fission, or with fission to form $\text{M}(\text{CO})_6$ and $\text{M}(\text{CO})_4$ (as has been proposed for photolytic polymerization-initiation reactions of $\text{Mn}_2(\text{CO})_{10}$ and $\text{Re}_2(\text{CO})_{10}$),²⁴ we consider these to be much less probable, the former because the nature of the solvent would ensure virtually complete ion pairing so that half-order kinetics would be most unlikely under any conditions, and the latter because there are no real grounds for postulating the electron-rich species $\text{M}(\text{CO})_6$ when evidence for the existence of five-coordinate 17-electron species is becoming much more convincing. This includes the studies of photochemical behavior²⁰ of $\text{Mn}_2(\text{CO})_{10}$ and $\text{Re}_2(\text{CO})_{10}$ (Wrighton et al. specifically reject the photochemical formation of $\text{M}(\text{CO})_6$ and $\text{M}(\text{CO})_4$) and the evidence¹⁹ for $\text{O}_2\text{Mn}(\text{CO})_{10}$. $\text{Mn}(\text{CO})_5$ and $\text{Re}(\text{CO})_5$ have been identified²⁵ in low temperature matrices, and an increasing number of well-authenticated substituted compounds of this type are being found.²⁶ We therefore consider the thermal, reversible, homolytic fission mechanism to be the best one available to account for our kinetic data with which it is in excellent qualitative and quantitative agreement.

The consequent assignment of ΔH_{11}^\ddagger and ΔH_{10}^\ddagger to homolytic fission of the Mn-Mn and Mn-Re bonds, respectively, provides a kinetic measure of their strengths. The observed correlations of these kinetic parameters, and of the corresponding ones for reaction of $\text{Tc}_2(\text{CO})_{10}$ and $\text{Re}_2(\text{CO})_{10}$ with oxygen, with spectroscopic parameters²³ related to the strengths of the metal-metal bonds, suggests that $\text{Tc}_2(\text{CO})_{10}$ and $\text{Re}_2(\text{CO})_{10}$ may also undergo thermal homolytic fission in their reactions with oxygen.

Acknowledgments. We are grateful to Erindale College and the National Research Council of Canada for support of this work, and to Mr. R. A. Jackson for performing some of the experiments.

References and Notes

- (1) Part IX. A. J. Poë and M. V. Twigg, *Inorg. Chem.*, **13**, 2982 (1974).
- (2) J. P. Fawcett, A. J. Poë, and M. V. Twigg, *J. Organomet. Chem.*, **51**, C17 (1973).
- (3) H. Wawersik and F. Basolo, *Inorg. Chim. Acta*, **3**, 113 (1969).
- (4) (a) D. Hopgood and A. J. Poë, *Chem. Commun.*, 831 (1966); (b) L. I. B. Haines, D. Hopgood, and A. J. Poë, *J. Chem. Soc. A*, 421 (1968).
- (5) L. I. B. Haines and A. J. Poë, *Chem. Commun.*, 964 (1968); *J. Chem. Soc. A*, 2826 (1969).
- (6) N. Filtrcroft, D. K. Huggins, and H. D. Kaesz, *Inorg. Chem.*, **3**, 1123 (1964); J. P. Fawcett, A. J. Poë, and M. V. Twigg, *J. Organomet. Chem.*, **61**, 315 (1973).
- (7) M. Basato and A. J. Poë, *J. Chem. Soc., Dalton Trans.*, 456 (1974).
- (8) L. I. B. Haines, Ph.D. Thesis, London University, 1968.
- (9) C. H. Bamford and R. Denyer, *Trans. Faraday Soc.*, **62**, 1567 (1966).
- (10) J. P. Fawcett, Ph.D. Thesis, London University, 1973, Chapter 4.
- (11) L. I. B. Haines and A. J. Poë, *Nature (London)*, **215**, 699 (1967); **218**, 562 (1968).
- (12) L. D. Segal, O. D. Krishevskaya, N. A. Belozerskii, N. E. Kolobova, and K. N. Anisimov, *Russ. J. Inorg. Chem.*, **12**, 592 (1967).
- (13) D. R. Bidinosti and N. S. McIntyre, *Can. J. Chem.*, **48**, 593 (1970).
- (14) C. H. Bamford and M. U. Mahmud, *J. Chem. Soc., Chem. Commun.*, 762 (1972).
- (15) R. A. Jackson, unpublished work.
- (16) M. Basato, J. P. Fawcett, and A. J. Poë, *J. Chem. Soc., Dalton Trans.*, 1350 (1974).
- (17) T. J. Morrison and F. Billet, *J. Chem. Soc.*, 2033 (1948).
- (18) J. Timmermans, "Physico-Chemical Constants of Pure Organic Compounds", Vol. II, Elsevier, Amsterdam, 1965, pp 170-173.
- (19) S. A. Fieldhouse, B. W. Fullam, G. W. Neilson, and M. C. R. Symons, *J. Chem. Soc., Dalton Trans.*, 567 (1974).
- (20) M. S. Wrighton and D. S. Ginley, *J. Am. Chem. Soc.*, **97**, 2065 (1975).
- (21) C. O. Quicksall and T. G. Spiro, *Inorg. Chem.*, **8**, 2363 (1969); T. G. Spiro, *Prog. Inorg. Chem.*, **11**, 17 (1970).
- (22) G. A. Junk and H. J. Svec, *J. Chem. Soc. A*, 1971 (1970).
- (23) J. P. Fawcett, A. J. Poë, and M. V. Twigg, *J. Chem. Soc., Chem. Commun.*, 2102 (1973).
- (24) C. H. Bamford and J. Paprotny, *Chem. Commun.*, 140 (1971).
- (25) H. Huber, E. P. Kündig, G. A. Ozin, and A. J. Poë, *J. Am. Chem. Soc.*, **97**, 308 (1975); E. P. Kündig and G. A. Ozin, *ibid.*, **96**, 5585 (1974).
- (26) R. H. Reiman and E. Singleton, *J. Organomet. Chem.*, **38**, 113 (1972); J. Moelwyn-Hughes, A. W. B. Garner, and N. Gordon, *ibid.*, **26**, 373 (1971); E. Singleton, J. T. Moelwyn-Hughes, and A. W. B. Garner, *ibid.*, **21**, 449 (1970); N. Freni, D. Giusto, and P. Romiti, *J. Inorg. Nucl. Chem.*, **29**, 761 (1967); F. Nyman, *Chem. Ind. (London)*, 604 (1965); R. S. Nyholm and D. V. Ramana Rao, *Proc. Chem. Soc., London*, 130 (1959).

Stereochemically Nonrigid Six-Coordinate Metal Carbonyl Complexes. II. ¹A ¹³C Nuclear Magnetic Resonance Study of the Series M(CO)₄(EMe₃)₂ (M = Fe, Ru, Os; E = Si, Ge, Sn, Pb)

Liviu Vancea, Roland K. Pomeroy, and William A. G. Graham*

Contribution from the Department of Chemistry, University of Alberta, Edmonton, Alberta, Canada T6G 2E1. Received July 16, 1975

Abstract: Carbon-13 NMR spectra are reported for the compounds M(CO)₄(EMe₃)₂ (M = Fe, E = Si, Ge, Sn; M = Ru or Os, E = Si, Ge, Sn, Pb) and for the chlorosilyl derivatives M(CO)₄(SiMe_{3-n}Cl_n)₂ (M = Fe, Ru, Os; n = 1-3). The study provides data on 19 *cis* isomers and 10 *trans* isomers. Spin-spin coupling in *cis* tin and lead derivatives leads to the assignment of the ¹³CO resonance at higher field as the equatorial carbonyl group; *cis*-Fe(CO)₄(SnMe₃)₂ is anomalous in this respect. Attention is directed to the averaging of axial and equatorial carbonyl signals in the *cis* isomers, which at room temperature results in a single carbonyl resonance for most of the iron derivatives. The barrier for this process increases with halogen substitution and is greater for corresponding compounds of ruthenium and osmium. The preservation of ^{117,119}Sn-¹³CO coupling in the high-temperature limiting spectrum of *cis*-Fe(CO)₄(SnMe₃)₂ shows that the process is nondissociative. The pattern of coalescence in *cis*-*trans* mixtures strongly suggests that axial-equatorial averaging proceeds by a *cis*-to-*trans*-to-*cis* isomerization process.

In 1972 we reported the results of a proton magnetic resonance study of the equilibrium mixture of *cis*- and *trans*-Os(CO)₄(SiMe₃)₂, which established that the isomers were rapidly interconverted on the NMR time scale at 55 °C.² The lack of exchange with ¹³CO suggested that the isomers were interconverted without dissociation, a process rarely observed in six-coordinate complexes.

It was anticipated that ¹³C NMR spectroscopy would play a key role in the continuation of these studies. Since axial and equatorial carbonyl groups of a *cis* tetracarbonyl derivative can be distinguished, any process which involves their interchange at an appropriate rate may be recognized. Thus, we have very recently shown that, in *cis*-Fe(CO)₄(SiMe₃)₂, there is rapid averaging of the signals due to axial and equatorial carbonyl groups (coalescence temperature -55 °C), and furthermore that the process does not involve ligand dissociation.¹

The trimethylsilyl derivatives of iron and osmium mentioned above provide important new examples of six-coordi-

nate polytopal rearrangement processes. In view of our interest in these processes and in factors governing the relative stabilities of *cis* and *trans* isomers, we have carried out an extensive ¹³C NMR study of compounds of this type and report here the results.

Experimental Section

NMR Instrumentation and Techniques. Spectra were recorded in the pulse Fourier transform mode of operation on a Bruker HFX-90-Nicolet 1085, or a modified Varian HA-100 spectrometer interfaced to a Digilab FTS/NMR-3 Data System and pulse unit. The instruments operated at 22.6 and 25.1 MHz, respectively.

The Bruker instrument, with which the majority of the spectra were obtained, was equipped with a single coil receiver; a pulse width of 6-8 μs (90° pulse = 27 μs) was used with a dwell time of 100 μs and an acquisition time of 0.8 s. Spectra were recorded using proton broad-band decoupling conditions. The number of scans was usually 1000 (1K). However, in the cases where exchange was observed or in order to determine coupling constants as many as 8- or 12K pulses were taken. The number of data points